



Chemical abundances determined from meteor spectra: I. Ratios of the main chemical elements

Josep M. TRIGO-RODRIGUEZ,^{1,2*} Jordi LLORCA,^{3,4} Jiri BOROVIČKA,⁵ and Juan FABREGAT⁶

¹Institute of Geophysics and Planetary Physics, UCLA, Los Angeles, California 90095–1567, USA

²Departament de Ciències Experimentals, Universitat Jaume I, 12071 Castelló, Spain

³Institut d'Estudis Espacials de Catalunya, Edifici Nexus, Gran Capità 2–4, 08034 Barcelona, Spain

⁴Departament Química Inorgànica, Universitat de Barcelona, Avgda. Diagonal 647, 08028 Barcelona, Spain

⁵Astronomical Institute, Czech Academy of Sciences, Ondrejov Observatory, 25165 Ondrejov, Czech Republic

⁶Observatori Astronòmic, Universitat de València, Edifici Instituts d'Investigació, Polígon La Coma, 46980 Paterna, València, Spain

*Corresponding author. E-mail: jtrigor@ucla.edu

(Received 2 December 2002; revision accepted 14 July 2003)

Abstract—Relative chemical abundances of 13 meteoroids were determined by averaging the composition of the radiating gas along the fireball path that originated during their penetration into the Earth's atmosphere. Mg, Fe, Ni, Cr, Mn, and Co abundances, relative to Si, are similar to those reported for CI and CM carbonaceous chondrites and interplanetary dust particles. In contrast, relative abundances of Ca and Ti in meteor spectra indicate that these elements suffer incomplete evaporation processes. The chemical composition of all meteoroids studied in this work differs from that of 1P/Halley dust.

INTRODUCTION

Objects responsible for fireballs are in the mass interval of $10^{-3} < m < 10^6$ kg (Hughes 1993) and come mainly from comets and asteroids. These bodies usually do not survive atmospheric interaction, especially when they enter the atmosphere at high velocity and are low density cometary fragments (Ceplecha et al. 1998). At present, the only way to obtain the heliocentric orbit of an incoming meteoroid is through monitoring the night sky for thousands of hours with all-sky cameras as part of a Fireball Network Programme (Ceplecha et al. 1998) or by obtaining casual video or satellite records (Brown et al. 2000). To date, only 7 meteorites have been recovered for which detailed data exists about their atmospheric trajectory and heliocentric orbit (Ceplecha 1961; McCrosky et al. 1971; Halliday et al. 1996; Brown et al. 1994, 2000; Spurný et al. 2002). Thus, meteor science is a valuable tool for gaining a better insight into the interplanetary material that reaches us. Recent Leonid campaigns brought together researchers from a wide range of disciplines and built a bridge between the observational and analytical sciences. Typically, fluffy cometary dust has been analyzed by cosmochemists through the study of interplanetary dust particles (IDPs) in the laboratory. Another discipline that addresses the study of this matter is meteor spectroscopy, which focuses on the light emitted during the process of ablation and fragmentation of

these particles in the atmosphere due to the high velocity at which they encounter with the Earth. Meteor spectroscopy provides interesting information about the ablation process and the chemical composition of incoming meteoroids. Although the first meteor spectra were registered in 1864 (Millman and Halliday 1961), little attention was devoted to meteor spectroscopy until several authors noted its intrinsic interest around the 1960s (Ceplecha 1961; Halliday 1961). In fact, before these authors' studies, meteor spectra interpretation was limited to the qualitative identification of the main lines in such spectra, without any physical interpretation being carried out.

Meteor phenomena consist of 3 differentiated parts: the head, the wake, and the train. The brightest region that surrounds the meteoroid, known as the meteor head, is the part that mainly contributes to spectra taken on photographic plates. Sometimes, the wake is also the origin of spectral lines that can be separated, as they belong to non-equilibrium processes. In 1964, Ceplecha developed a complex cylindrical model for the radiating column, assuming the existence of local thermal equilibrium. Using this model, the theoretical curve of growth was built up taking into account the self-absorption of the lines and other physical parameters. But, the resulting number of iron atoms in the radiating volume and the mass of this volume as determined from the known luminous efficiency of meteors were not always

accurate. Borovička (1993) tested a simpler model on the excellent Cêchtice fireball spectrum and obtained, for the first time, a synthetic computer-created meteor spectrum. Although the physical approach was very simple, it matched the observed spectrum exceptionally well: thermal equilibrium and constant temperature and density throughout the whole volume. Here, we follow the same procedure and use the software developed by Borovička (1993). We have computed a synthetic spectrum for each fireball and compared it with the observed spectrum. The model considers the radiating volume to be a prism where physical parameters and chemical abundances can be determined. It assumes thermal equilibrium in the meteor head, an acceptable approach during the short time in which the intense radiation that is registered on the photographic plate is produced. The validity of the thermal equilibrium assumption has also been supported recently from the theoretical point of view (Boyd 1998). On the other hand, Borovička (1994) has pointed out that all meteor spectra consist of 2 different components: the main spectrum characterized by a temperature of about 4500 K and a second spectrum that usually reaches 10000 K. The second component originates in the front wave where high-energy collisions can produce the excitation of atoms, thus, increasing the ionization of the meteoroid components. Here, we provide more evidence to support this idea.

This paper attempts to derive relative chemical abundances of incoming meteoroids from the spectroscopic analysis of the luminous trajectories produced during their entry into the terrestrial atmosphere. Here, we analyze the averaged abundances for the main chemical elements in meteor spectra. First, we describe the observational methodology and data reduction. Then, we explain the model used to derive the chemical abundances relative to silicon. And, finally, we discuss the implications of the abundances

that were calculated for the fireballs analyzed and compare them with other solar system objects. In an additional work (Paper II), we focus in detail on the main implications of the derived Na/Si ratios.

METHODOLOGY

We analyzed 15 meteor spectra belonging to 13 different fireballs registered at the Ondrejov Observatory between 1961 and 1989 (Table 1). All spectral records were obtained with fixed cameras equipped with prisms or diffraction gratings. Ten of them were obtained using a prism to scatter meteor light, and the others were obtained using a diffraction grating with 600 grooves/mm. The focal length of the camera was 360 mm and the focal ratio 1:4.5. The typical exposure time was several hours on 2 different films. Older spectra with codes GEM, PER1, and PER2 were registered on 18×24 cm AGFA 100 plates, while the other spectra were taken on ORWO NP27 (400 ASA) plates of identical size. The spectral plates were measured in detail using a 2-axis CSPC-2000 densitometer from the French company Composants et Systèmes de Précision. The camera plates were scanned along the diffraction hyperbola since the meteor paths were often out of the optical axis of the camera (Cepplecha 1961). To obtain a detailed analysis, the densitometer included a rotation slot for keeping the measured signal window perpendicular to the meteor path. The slot dimensions were adapted to each spectrum according to the apparent size of the brightest lines. The spectra were scanned at least once per segment, but often more frequently, depending on the slot size. The wake was also measured between segments to determine the plate background and its influence on each spectrum. The exact location of the scans were marked on photographs, as shown in the AND spectrum (Fig. 1). Scans

Table 1. Spectra analyzed in this work. We give the number of the Ondrejov Observatory spectra catalog, the code assigned in this work, and the date when the spectra were taken. The geocentric velocity and the most significant orbital parameters are given, i.e., the semimajor axis and inclination of the heliocentric orbit of the parent meteoroid. N.S. means the number of segments that were analyzed to deduce the averaged abundances. The last column gives the approximate photometric mass in grams, which was obtained using Verniani's (1973) formula.

Ondrejov catalog	Code	Date	Stream	V_g (km/s)	a (AU)	i (°)	Type	N. S.	Mass (g)
562	GEM	December 14, 1961	Geminid	37.8	1.7	39	Grating	16	4
774	PER1	August 2–3, 1962	Perseid	59.9	23.0	112	Prism	4	(0.2)
3975	PER2	August 12–13, 1967	Perseid	60	11	113	Prism	1	(1)
5435	PER3	August 11–12, 1969	Perseid	60.9	250	114	Prism	10	(4)
5438	PER4	August 11–12, 1969	Perseid	60.7	19.0	114	Prism	19	(29)
6021	SPO2	June 6–7, 1970	Sporadic	26.4	3.0	39	Prism	6	(56)
6135	PER5	August 12–13, 1970	Perseid	60.6	115	113	Prism	11	(6)
6701/6703	KCIG1–1r	August 18–19, 1971	Cignid	25.6	4	36	Prism/Grating	2/4	(600)
8864	SPO1	September 17–18, 1974	Sporadic	68	∞	148	Prism	13	21
11274	AND	October 8–9, 1977	Andromedid	24.3	2.9	4	Prism	16	4000
14631	LEO	November 17–18, 1980	Leonid	72.4	13	162	Prism	9	250
20271 + 20273	SPO3-3r	November 30 to December 01, 1989	Sporadic	25.6	2.4	5	Prism/Grating	18/6	(9000)
90011	SPO4	May 19–20, 1974	Sporadic	57.1	12.9	103.9	Prism	16	(2)

were labelled with letters; the brightest part was labelled as segment A and the other scans were named in growing and decreasing order. All the spectra analyses and scans are available in Trigo-Rodríguez (2002).

The measurements were carefully calibrated according to the relative spectral sensitivity of the spectrograph. The wavelength scale for each spectrum was determined by means of known lines in the spectrum (Borovička 1993). Plate sensitivities were obtained to calibrate the real intensity of each line due to the fact that the plate response was different at each wavelength. The plate sensitivity of old plates taken on AGFA 100 was obtained by studying the bright, detailed spectra of the star Polaris. These spectra were recorded on the same plate as the GEM spectrum (Fig. 2). First, the linear part of the characteristic curve of the GEM plate was constructed

by scanning the zero order spectra of all stars recorded, excluding the red and variable stars (Fig. 3). Then, the first and second orders of the Polaris spectrum were scanned. The wavelength scale was determined by means of known emission and absorption lines in the stellar spectrum. To relate the instrumental lengths to wavelengths, we used a polynomial of degree 3. The real energy distribution in the Polaris spectrum was calculated using the Kurucz (1991) atmosphere models implemented within the DIPSO package of the Starlink software collection (Howart et al. 1996). We used the following astrophysical parameters to model the flux of the Polaris star: $T_{\text{eff}} = 5000$ K, $\log g = 2.1$ and $E(B-V) = 0$. All these data were taken from Andrievsky et al. (1994). The real energy distribution obtained for this star was compared with the measured spectrum (transformed into the relative spectral flux



Fig. 1. The Andromedid spectrum (AND) analyzed in this work. The spectrum is divided into segments due to the rotating shutter.

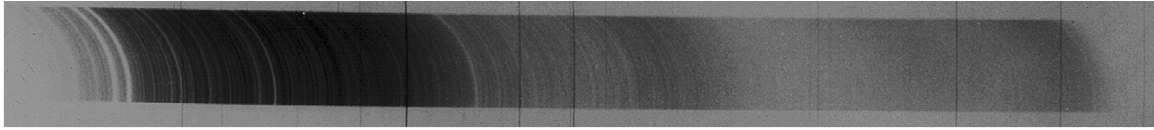


Fig. 2. The Polaris spectrum registered on the GEM plate.

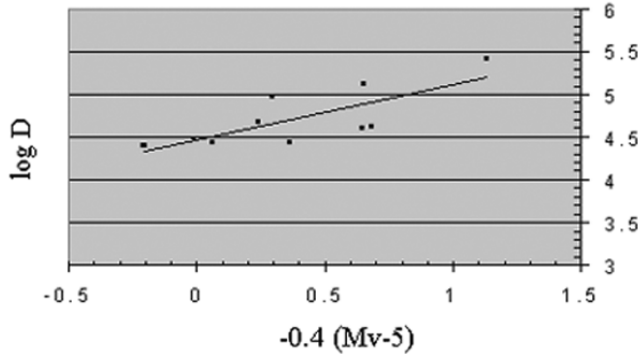


Fig. 3. Characteristic curve of the GEM plate.

by means of the characteristic curve). The ratio of both yielded the relative spectral sensitivity function, which provides us with the plate response for each wavelength. For the spectra taken on ORWO NP27, we assumed the spectral sensitivity obtained by Borovička (1993) by analyzing the Saturn spectrum on the plate of the Cechtice fireball. Both sensitivity curves are shown in Fig. 4. Precise photometric measurement of the meteor trails allowed us to obtain the absolute magnitude of the fireballs. In the Ondrejov Observatory, the photometry was performed from all-sky images, which enabled us to compare the fireball magnitude relative to the stars by taking into account their different angular velocity in the sky (see Rendtel [1993] for a detailed explanation).

The absolute calibration of the spectra consisted of, basically, adjusting the flux arriving from the meteor using the following equation:

$$F(\lambda) = A \times c^{-1}(\lambda) \times (D[\lambda])^p \quad (1)$$

where D is the measured opacity, p is the reciprocal slope of the characteristic curve, c is the spectral sensitivity function, and F is the absolute energy flux. The absolute magnitude of the fireball is adjusted by changing the (A) value until the magnitude agrees with the measured magnitude of the fireball estimated from all-sky images. Unfortunately, the absolute magnitudes of some fireballs were not available, so absolute calibration was not always possible. In these cases, we assumed a typical value for the absolute calibration constant of $A = 10^9$. In this work, however, we consider relative elemental abundances, which, in turn, are not affected seriously by the absolute calibration (Borovička 1993).

We used the empirical equation deduced from 6000 radio meteors by Verniani (1973) to relate the photometric magnitude and the geocentric velocity of the meteors with the mass of the incoming meteoroids:

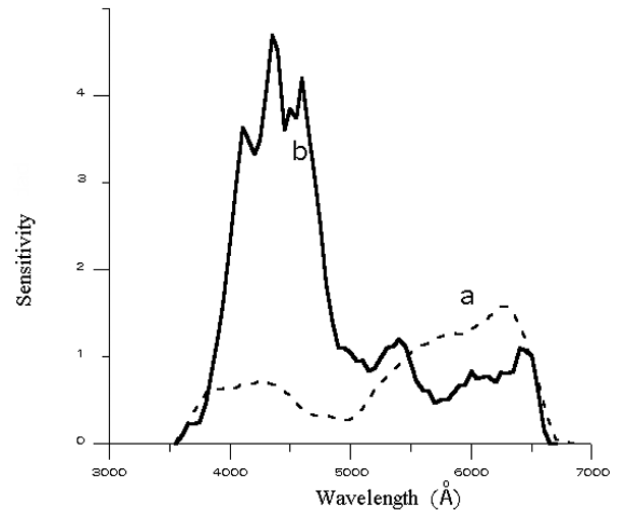


Fig. 4. Spectral sensitivity of the 2 types of plates used here to obtain meteor spectra.

$$0.92 \times \log m(g) = 24.214 - 3.91 \times \log V_g(\text{cm/s}) - 0.4 \times M_v \quad (2)$$

where m is the meteoroid mass in grams, V_g is the geocentric velocity given in cm/s, and M_v is the visual magnitude of the meteor.

Results are given in the last column of Table 1. We have estimated the mass uncertainty to be $\sim 10\%$ for fireballs with a known absolute magnitude and $\sim 30\%$ when the absolute magnitude is not known (given between parentheses in Table 1).

To obtain the relative chemical composition of meteoroids, we used the geometrical model of the meteor developed by Borovička (1993). The radiating volume is treated as a prism with a square base and elongated in the direction of the meteor flight. The prism length is (b) and the width is (a). The model assumes, for the sake of simplicity, that the spectrograph only sees one side of that prism (see Fig. 5). The angle between the side of the prism and the observer was calculated for each fireball from the known meteor trajectory in space. The b/a ratio of the meteor radiating head could not be determined from photographic observations due to a low resolution and the fact that the meteor spectra moved too quickly along the plate in the exposure interval. Only an upper limit for (a) was obtained from the width of the meteor trail in the photograph. Assuming thermal equilibrium, the brightness of the spectral lines were computed by adjusting 4 parameters: temperature (T), the column density of atoms (N), the damping constant (Γ), and

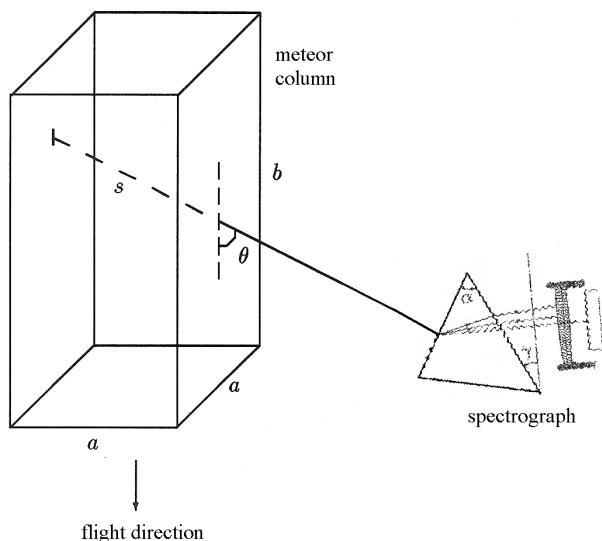


Fig. 5. Diagram of the geometrical model of the radiating head assumed for density determinations.

the surface area (P) (Borovička 1993). The surface area registered by the spectrograph is:

$$P = a \times b \times \sin\theta \quad (3)$$

From this equation, we estimate the approximate b/a ratio for the analyzed photographs, the resulting values being between 0.5 and 4. In consequence, we assumed the value of the b/a ratio to be 2 for all spectra, as proposed Borovička (1993). We will discuss the influence of this assumption in the final results.

The procedure was to use a software application to reconstruct a synthetic spectrum that enabled us to determine these 4 parameters from the observed brightness of lines (see Fig. 6). This is done by the least square method implemented on the software. As most lines in the spectrum are of neutral iron, Fe I is taken as a reference element to adjust the intensity of lines and temperature. When T , Γ , and P have been estimated, the software enables us to change the column density (N) of any element. To obtain the chemical composition, the degree of ionization of different elements must be considered, taking into account the ratio of neutral, singly, and doubly ionized atoms given by the Saha equation. A more detailed explanation of the full procedure and the related theory is given in Borovička's (1993) original paper.

RESULTS AND DISCUSSION

The Contribution of the Two Spectral Components

One important discovery by Borovička (1993) was that meteor spectra consist of 2 separate components produced at very different temperatures. The main spectrum has a temperature that usually varies between 4000 and 5000 K and

contains most of the spectral lines. A second component with a typical temperature around 10000 K is also present and consists of a few lines of ionized elements, especially Fe II, Mg II, Ca II, and Si II.

Following the procedure explained by Borovička and Betlem (1997), we determined the ratio of Fe atoms contributing to both spectral components. From Table 2 one can observe that as the geocentric velocity becomes higher, the temperature of the main component increases, as well as the number of ionized atoms contributing to the second component. This is probably due to the faster movement of the meteoroid through the atmosphere, which results in an increase in the excitation temperature of the surrounding gas.

As can be seen in Table 2, for all the fireballs analyzed, most of the mass contributes to the main component. The M_1/M_2 ratio decreases when the geocentric velocity rises, showing that the temperature and abundance of Fe atoms contributing to the high temperature component also increase. Table 3 shows how the different temperatures of both components have a direct effect on the percentage of neutral and ionized atoms for the different elements, this being the reason that the second component is characterized by lines of ionized elements. We must also point out that this high temperature component has an Fe atomic density in the meteoric column that is lower than that of the main component, despite having higher temperatures. In general, the Fe atomic density for the second component is around 10^{14} atoms/cm⁻², although in high velocity meteoroids, this typical density can be larger. These results support the idea that the high temperature component is generated in the collision front of the meteoroid. On the other hand, from Table 2, one can also observe that the temperature of the second component appears to be velocity-independent.

Testing the Determination of Relative Chemical Abundances

Before giving the values of relative chemical abundances in meteor spectra, we first offer a critical discussion of their determination. To test the model and compare the results obtained from prism and grating spectra, we decided to determine the relative chemical abundances of 2 fireballs obtained from more than one spectrograph. The reason for this is that, for 2 fireballs (KCIG and SPO3), we had duplicate spectra: one prism and one grating spectrum. The comparison of both results obtained independently can be very useful in testing the consistency of the methodology used in determining abundances. The resolution of the prism was 130 Å/mm at 4000 Å and 550 Å/mm at 6000 Å, while that of the grating spectra was 50 Å/mm for all wavelengths.

In Table 4, we can see that close values were obtained for KCIG-KCIGr and SPO3-SPO3r, which shows that real uncertainties are probably smaller than those obtained when taking the abundance dispersion along the meteor trail into

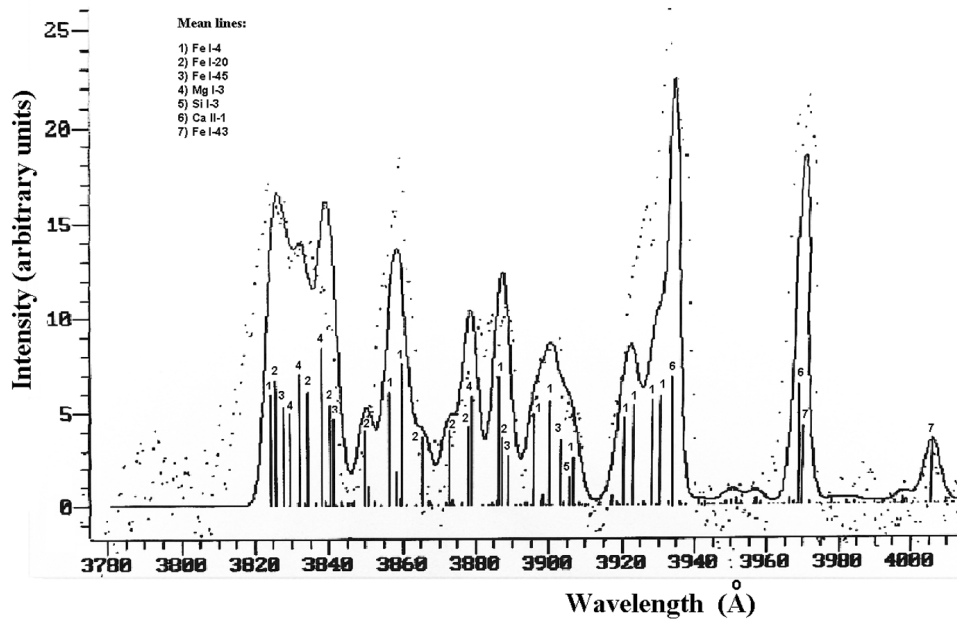


Fig. 6. Observed spectrum (dotted line) and the synthetic spectra (continuous line) obtained from the determination of physical parameters, following the method explained in the text. The spectrum belongs to fireball SPO3r in the 3780–4010 Å wavelength interval, where the main lines are identified. The synthetic spectra is the sum of the lines coming from the main and the second component at 4800 and 9500 K, respectively.

Table 2. Mass ratio between the main component (M_1) and the high temperature component (M_2) for some fireballs analyzed with representative geocentric velocities. For this estimation, we took the brightest point of the fireball trajectory. The temperature and the density of Fe atoms in the column for the main component (ρ_1) and the high temperature (ρ_2) are included. N_{Fe} and N_{FeII} represent the number of Fe atoms contributing to the main and second component, respectively.

Spectrum	Vg (km/s)	H (km)	M_{abs}	T_1 (K)	$\rho_1 \times 10^{14}$ (cm^{-2})	T_2 (K)	$\rho_2 \times 10^{14}$ (cm^{-2})	$N_{\text{Fe}} \times 10^{19}$	$N_{\text{FeII}} \times 10^{19}$	M_1/M_2
AND	23.1	66.1	−8.9	4300	2	(9500)	1	449	3	150
KCIGr	23	(85)	−8.5	4600	5	(10000)	1	510	2	300
SPO3r	29	–	(−8)	4900	10	(9500)	1	1250	50	250
GEMr	38	–	(−5)	4500	2	(9500)	1	2	0.1	20
SPO4	57	79.0	−6	4800	5	(10000)	1	6	3	2
PER2	60	(95)	(−8)	4400	5	(10000)	1	10	1	10
SPO1	67.8	96	(−12)	5800	50	(10000)	5	593	92	6
LEO	71.9	89.8	−10	5700	10	(10000)	5	350	63	6

account. Bear in mind, the chemical composition of the radiating gas in a fireball varies along its path and it can exert an influence reflected in the overestimation of relative errors.

Relative Chemical Abundances

From the comparison of the synthetic and observed spectra along several points in the trajectory of the 13 fireballs, we have obtained the abundance ratio relative to silicon for several elements. In the spectra produced by high geocentric velocity meteors, we can obtain the silicon abundance directly from the second component of the spectra, where Si II lines are very prominent. Unfortunately, for slow

meteors, we cannot determine the Si abundance based on their spectra. For these meteors, the second component is very faint and Si II is usually missing. Moreover, higher resolution spectra are needed to separate the contribution of the Si I line (multiplet 3 at $\lambda = 3905.5$ Å), which is located in a spectral region where Fe I and Ca II lines are very prominent. In these cases, we assumed a typical chondritic ratio of $\text{Si/Fe} = 1.16$ (Anders and Grevesse 1989).

Here, we give only the averaged abundance for each fireball along its trajectory. The composition of each fireball was measured in more than 10 segments, but the exact number of selected segments depended on the characteristics of each fireball. The exact number of segments averaged in

Table 3. Main elements in the meteor column, assuming a chondritic composition and typical composition of the atmospheric gas. The assumed percentage of each chemical element is given in the second column. The percentage of neutral (E I) and ionized (E II) atoms in the meteoric gas are given for 3 typical temperatures.

Element	Assumed abundance	4000 K		5000 K		10000 K	
		% E I	% E II	% E I	% E II	% E I	% E II
H	6	100	0	100	0	74.8	25.2
C	0.90	100	0	100	0	24	76
N	60	100	0	100	0	81.1	18.9
O	30	100	0	100	0	87.6	12.4
Na	0.07	8.5	91.5	1.8	98.2	0	100
Mg	1.18	97.1	2.9	60.2	39.8	0.2	96.9
Al	0.09	75.9	24.1	27.3	72.7	0.3	99.6
Si	1.16	99.8	0.2	94	6	0.9	98.9
S	0.56	100	0	100	0	13.4	86.6
Ca	0.07	28	72	4.1	95.9	0	46
Cr	0.02	85.8	14.2	31.4	68.6	0.1	98.0
Mn	0.01	96.9	3.1	61.3	38.7	0.2	97.3
Fe	1.00	98.7	1.3	74.6	25.4	0.2	98.2
Ni	0.06	99.6	0.4	91.1	8.9	1.1	98.6

Table 4. Chemical abundances as regards Si compared with those typical of other solar system bodies. The data between parentheses are approximate. P/Halley represents the averaged abundance of the dust particles of the comet 1P/Halley (Jessberger et al. 1988).

Esp.	Ca ($\times 10^{-3}$)	Mn ($\times 10^{-4}$)	Ti ($\times 10^{-4}$)	Mg	Na	Cr ($\times 10^{-3}$)	Ni ($\times 10^{-3}$)	Fe	Co ($\times 10^{-4}$)
GEMr	15 \pm 8	49 \pm 17	–	0.90 \pm 0.13	0.09 \pm 0.03	7 \pm 3	–	–	–
PER1	39 \pm 31	25 \pm 18	–	1.08 \pm 0.30	0.08 \pm 0.02	10 \pm 5	–	0.84 \pm 0.13	–
PER2	18	29	(18 \pm 7)	0.88	0.07	8 \pm 4	–	0.71	–
PER3	27 \pm 16	73 \pm 31	–	0.85 \pm 0.36	0.08 \pm 0.03	9 \pm 7	–	0.87 \pm 0.35	–
PER4	60 \pm 31	54 \pm 19	(35 \pm 23)	0.97 \pm 0.23	0.11 \pm 0.02	11 \pm 6	(15 \pm 4)	0.98 \pm 0.25	–
SPO2	11 \pm 9	71 \pm 17	–	0.39 \pm 0.15	0.11 \pm 0.04	11 \pm 3	–	–	–
PER5	21 \pm 9	44 \pm 22	(24 \pm 10)	0.83 \pm 0.33	0.07 \pm 0.04	8 \pm 5	(34 \pm 22)	0.87 \pm 0.09	–
KCIG1	7 \pm 1	39 \pm 15	–	1.04 \pm 0.03	0.07 \pm 0.04	5 \pm 2	–	–	–
KCIG1r	11 \pm 4	34 \pm 21	(16 \pm 5)	0.95 \pm 0.19	0.08 \pm 0.02	6 \pm 1	–	–	–
SPO1	24 \pm 10	58 \pm 25	(17 \pm 4)	0.91 \pm 0.30	0.10 \pm 0.08	8 \pm 5	(15 \pm 10)	0.80 \pm 0.43	–
AND	13 \pm 4	89 \pm 20	(34 \pm 10)	0.85 \pm 0.24	0.08 \pm 0.04	8 \pm 3	(16 \pm 4)	–	(20 \pm 5)
LEO	26 \pm 20	73 \pm 25	18 \pm 4	0.79 \pm 0.48	0.08 \pm 0.02	4 \pm 1	–	0.81 \pm 0.26	(40 \pm 5)
SPO3	24 \pm 13	62 \pm 26	(17 \pm 6)	0.89 \pm 0.24	0.08 \pm 0.05	6 \pm 5	(23 \pm 13)	–	(19 \pm 6)
SPO3r	36 \pm 8	72 \pm 18	(18 \pm 3)	1.06 \pm 0.15	0.08 \pm 0.01	6 \pm 3	21 \pm 9	–	(13 \pm 8)
SPO4	37 \pm 26	57 \pm 23	(16 \pm 6)	0.61 \pm 0.20	0.09 \pm 0.04	6 \pm 3	(25 \pm 10)	0.91 \pm 0.07	–
P/Halley	34	30	20	0.540	0.054	50	220	0.280	–
CI	71	90	20	1.06	0.060	13	51	0.900	–
CM	72	60	20	1.04	0.035	12	46	0.84	–
IDPs	48	150	20	0.85	0.049	12	37	0.63	–

each fireball is given in Table 1. The individual results for each segment are given in Trigo-Rodríguez (2002). The final averaged values for the fireball trajectories are shown in Table 4.

From Table 4, we can deduce that the main composition of the meteoroids is, in general, more similar to IDPs than to chondritic values. This supports the cometary origin of IDPs because most of these particles are associated to comets, as is deduced from the calculated fireball orbits (Trigo-Rodríguez 2002). This is interesting since all the meteoroids associated with these fireballs were larger than the typical size of IDPs. Another important result is reached when comparing the estimated abundances with that of 1P/Halley dust. Table 4

gives the abundances measured by the Giotto spacecraft spectrometers, which are significantly different from our values. To explain these differences, we suspect that, on their approach to the comet nucleus, Giotto spectrometers only detected small particles with a mean composition probably very different to larger particles (Rietmeijer, personal communication). Moreover, the recently analyzed Halley particles may show important differences with cometary meteoroids because of the very different exposure time to solar radiation in the interplanetary medium. In fact, according to Hughes (1993), the meteoroids belonging to a stream need thousands of years to lose their orbital similarity to their parent bodies. When this occurs, these old meteoroids are said to be

sporadic. For this reason, we find it interesting to compare our sample of sporadic meteoroids with the sample of cometary meteoroids. Sporadic meteors are closely connected to IDPs because the survival of IDPs is usually associated with low velocity entries. In fact, Greenberg (1998) proposed that the differences between cometary meteoroids and IDPs were related to their permanence in the interplanetary medium. Most IDPs have probably been orbiting the sun for hundreds of thousands of years, while the age of cometary meteoroids can be measured in centuries. In this long voyage around the inner solar system, these particles are altered by solar radiation, i.e., by the removal of their volatile component.

The Analysis of Individual Ratios

Figure 7 shows the relative chemical abundances plotted against the geocentric velocity.

Na/Si

In general, we found that the sodium ratio (Na/Si) is larger than that of typical chondritic meteorites and IDPs (Rietmeijer and Nuth 1998), but it is also higher than the sodium content in the dust of 1P/Halley (Jessberger et al. 1988). These results support the hypothesis that this volatile element is probably partially removed from a volatile cover and/or from the mineral matrix during its entry into the atmosphere and also during its stay in the interplanetary medium. We have dedicated Paper II to a more detailed discussion of this finding. In that study, we prove that the observed Na does not belong to the terrestrial atmosphere and has not been overestimated due to our assumptions in the model used to determinate abundances.

Mg/Si

For this element, the values are inside those expected for IDPs and chondrites but are, in general terms, a long way from those of the 1P/Halley dust composition (Jessberger et al. 1988). The fact that 2 sporadic meteors, SPO2 and SPO4, have low Mg abundances compared to the others is very significant. The 2 meteoroids had masses of only 56 and 2 g, respectively. These particles had an anomalous chemical composition, which was probably due to mineral phases with a poor Mg content.

Ca/Si

Calcium is present in refractory mineral phases that have a special resistance to volatilization. Totally unambiguous Ca lines are clearly visible in all meteor spectra. In the main component, the Ca I line belonging to multiplet 2 is always apparent at 4227 Å. Moreover, the lines of the Ca II doublet originated by multiplet 1 appear at 3934 and 3968 Å, which are also clearly visible, especially in the case of high velocity meteoroids. These 2 lines overlap the contribution of the high temperature component that converts these lines into the most

prominent in all spectra, especially for low velocity meteors. In Fig. 7, we can see the clear dependence between the observed Ca abundance and the geocentric velocity of the meteoroids. The explanation for this lies in the effect exerted by incomplete evaporation first proposed by Borovička (1993, 1994b). When the geocentric velocity increases, the main temperature reached in the meteoric column also increases. Due to the location of Ca in refractory phases, the higher the temperature is, the more efficient volatilization is and, consequently, the greater its contribution to the luminous spectra. On the whole, we can see that, for meteoroids with a geocentric velocity between 20 and 40 km/s, the effect of incomplete evaporation causes only ~30 or 50% of the calcium to contribute to the luminous spectra. For fast meteors, the observed contribution made by calcium can attain higher values but rarely reaches the expected values for IDPs or chondritic meteorites. The heterogeneity of the particles can also affect results. For example, the geocentric velocity of the 5 Perseids (PER) analyzed is nearly identical, but their calcium content differs. More specifically, PER4, a particle with a weight of around 29 g, is far richer in calcium than the others, which probably shows that a rich Ca phase was present in its structure.

Ti/Si

Titanium is a minor element that, in meteor spectra, has several lines along the main spectrum and also in the high temperature component. The brightest line of Ti I usually appears at 4982 Å and at 4550 Å in the case of Ti II. Unfortunately, these lines are close to Fe lines and are very faint. Consequently, the Ti abundance has been deduced in the brightest meteor segments to avoid confusion with other lines and noise. In general terms, the results shown in Fig. 7 are around the expected values for IDPs and chondritic meteorites.

Cr/Si

Chromium is a transition element that is very easy to identify in meteor spectra because its multiplet 1 has 3 intense lines at 4254, 4275, and 4290 Å. Moreover, multiplet 7 generates 1 line that is also visible around 5206 Å. Cr abundance is determined directly by adjusting the synthetic spectrum to the multiplet 1 lines, which is an excellent reference that allows us to obtain a high degree of accuracy in the determination of elemental abundances of chromium. The abundance in Cr for all meteoroids is generally observed to lie between the typical values of IDPs, chondritic meteorites and 1P/Halley dust. We note that 109P/Swift-Tuttle meteoroids (PER1–5) are richer in this element than, for example, sporadic meteoroids. Also, remarkably, the Leonid fireball (LEO) had a very low Cr/Si ratio, similar to that measured for the 1P/Halley dust.

Mn/Si

This element is also easy to identify in meteor spectra. Multiplet 1 has an important line at 4033 Å and other

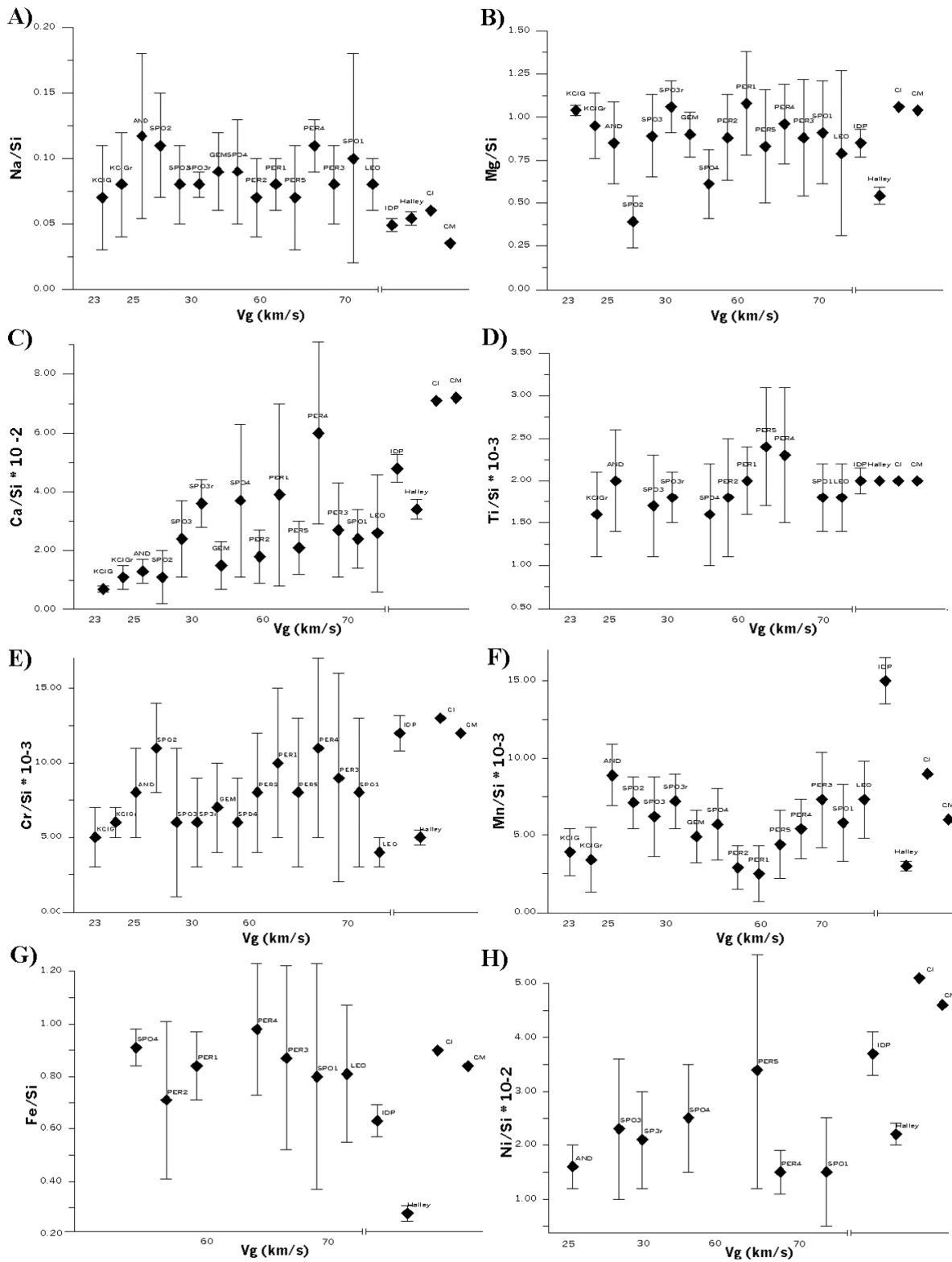


Fig. 7. Relative chemical abundances. The spectra are ordered according to their geocentric velocity. For comparison, the expected ratios for IDPs, CI and CM chondrites, and 1P/Halley dust are also included: a) Na/Si; b) Mg/Si; c) Ca/Si; d) Ti/Si; e) Cr/Si; f) Mn/Si; g) Fe/Si; and h) Ni/Si.

Among the elements that were present in the primeval inner solar nebula, Si, Mg, and Fe were the most abundant. Their individual behavior at high temperatures probably accounts for their different abundances in the bodies condensed there (Ozawa and Nagahara 2000). These 3 chemical elements are the major components of inner solar system bodies because we accept the fact that all of them were formed from the condensation of a vapor rich in Mg-Fe-SiO-H₂-O₂ and little silicate particles that made up the protoplanetary nebula 4.5 My ago (Rietmeijer and Nuth 1998). Consequently, the relative proportion of these 3 elements is usually a good tool with which to find possible relationships between different objects. Figure 9 shows the Mg-Fe-Si ternary diagram where the chemical similarity between the meteoroids producing the spectra analyzed in this work and the IDPs and chondritic meteorites is, again, implicit. All spectra are clustered between the typical IDPs and chondritic values, except for 2 sporadic meteoroids (SPO2 and SPO4), which are poor in Mg. Note that both meteoroids are the only ones that are close to the Mg abundance of 1P/Halley dust, although their Fe and Si contents are different. But, are the particles of this comet really anomalous or could this be an artefact of the measurements? To answer this we must state that, by combining the mass and the composition of each particle detected by the Giotto mass spectrometers, Fomenkova et al. (1992) concluded that the dust of this comet is made up of 3 kind of particles: 1) the so called CHON particles; 2) particles that are rich in carbonaceous compounds and silicates; and 3) mineral particles with Fe, Mg, and Si as their main components. Note that the CHON particles have not been recovered until now in the terrestrial atmosphere probably because of their fragility to the solar radiation during their stay in the interplanetary medium or, as was suggested by Rietmeijer (2002), due to their being fused during their fast entry into the terrestrial atmosphere. The Halley mass spectrometers detected only very small particles that have masses equivalent to the so called principal components (PCs) which are inside the matrix of IDPs. Neither PCs nor any other constituent (e.g., mineral grains) has chondritic element proportions (Rietmeijer 1998). In consequence, the Giotto measurements were biased towards small cometary particles and, from our results, we conclude that they are not representative of other cometary particles reaching the earth.

CONCLUSIONS

Meteor spectroscopy can be used as a valuable tool for comparing the chemical abundances between meteor streams and their respective parent bodies. Using meteor spectroscopy to deduce the elemental chemical abundances in meteoroids has enabled us to draw the following conclusions:

1. All the meteor spectra analyzed are characterized by 2 spectral components: a main component with a temperature around 4000–5000 K and a second high temperature component that usually reaches 9500–

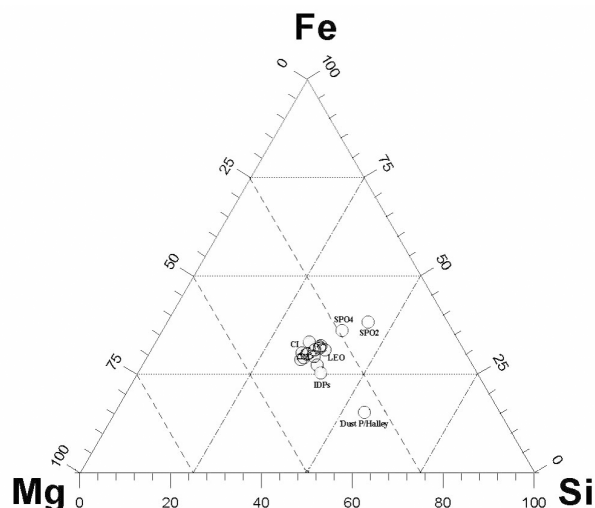


Fig. 9. Mg-Fe-Si ternary diagram for the analyzed spectra. For comparison, the position in the diagram of IDPs, CI chondrites, and the dust of 1P/Halley are also plotted.

10000 K. The main component is characterized by the presence of lines associated with the meteoroid components: Fe I, Mg I, Ca I, Ca II, Al I, Ti I, Mn I, Cr I, and Na I. The second component shows lines associated with the meteoroid composition: Fe II, Ca II, Mg II, Ti II, Si II, and Mg II but also presents N II and O II lines coming from atmospheric elements.

2. The second and main component can be adjusted reasonably well if thermal equilibrium is assumed and it is compared with synthetic spectra to obtain relative chemical abundances in the meteor columns.
3. Na is the most volatile of all observable elements detected by photographic meteor spectroscopy. This element is usually volatilized very quickly and is almost missing at the end of the fireballs, even when meteoroid fragmentation provides fresh Na embedded in the mineral matrix.
4. The results support the supposition that cometary meteoroids have a chemical composition very similar to that found in collected IDPs. We know that the collected 10 micron-sized fluffy IDPs survive in a range of 11 to ~25 km/s, which includes sporadic meteors as well as dust associated with near-earth asteroids (NEAs) and low velocity cometary meteoroids probably associated with extinct and dormant comet nuclei. But, the process is not as straightforward for cometary particles with larger entry velocities that are disintegrated and hardly degraded in the atmosphere during the ablation process. In any case, we have found a chemical similarity that supports the proposed origin of IDPs in comets and their link with other high-velocity particles that have eluded laboratory analysis.
5. The differences of the 1P/Halley dust composition reveal that particles from this comet have a very different

chemical composition compared to other cometary particles. In fact, our results support the idea that the Giotto measurements of the 1P/Halley dust cannot be considered as representative of all cometary meteoroids, as has been suggested (Jessberger et al. 1988b).

Acknowledgments—J. M. Trigo-Rodríguez was encouraged by discussions with Mayo Greenberg (Leiden University) prior to this work. J. Llorca is grateful to MCYT for a Ramon y Cajal Research Program. J. M. Trigo-Rodríguez is grateful to the Spanish State Secretary of Education and Universities for a postdoctoral grant.

Editorial Handling—Dr. Beth Ellen Clark

REFERENCES

- Abe S., H. Yano, Ebizuka N., and Watanabe J. I. 1998. First results of high-definition TV spectroscopic observations of the 1999 Leonid shower. *Earth, Moon, and Planets* 82–83:369–377.
- Anders E. and Grevesse N. 1989. Abundances of the elements: Meteoritic and solar. *Geochimica et Cosmochimica Acta* 53:197–214.
- Andrievsky S. M., Kovtyukh V. V., and Usenko I. A. 1994. The chemical composition of the s-Cepheids. I Alpha Ursae Minoris (Polaris) and HR 7308 (V473 Lyrae): Unique Cepheids of the Galaxy. *Astronomy and Astrophysics* 281:465–470.
- Borovička J. 1993. A fireball spectrum analysis. *Astronomy and Astrophysics* 279:627–645.
- Borovička J. 1994. Two components in meteor spectra. *Planetary and Space Science* 42:145–150.
- Borovička J. 1994b. Line identifications in a fireball spectrum. *Astronomy and Astrophysics Supplement Series* 103:83–96.
- Borovička J. 1999. Meteoroids properties from meteor spectroscopy. In *Meteoroids 1998*, edited by Baggaley W. J. and Porubcan V. Bratislava: Slovak Academy of Sciences. pp. 355–362.
- Borovička J. and Betlem H. 1997. Spectral analysis of two Perseid meteors. *Planetary and Space Science* 45:563–575.
- Borovička J. and Jenniskens P. 1998. Time resolved spectroscopy of a Leonid fireball afterglow. *Earth, Moon, and Planets* 82–83:399–428.
- Borovička J., Stork R., and Bocek J. 1999. First results from video spectroscopy of 1998 Leonid meteors. *Meteoritics & Planetary Science* 34:987–994.
- Boyd I. D. 1998. Computation of atmospheric entry flow about a Leonid meteor. *Earth, Moon, and Planets* 82–83:93–108.
- Brown P., Ceplecha Z., Hawkes R. L., Wetherill G., Beech M., and Mossman K. 1994. The orbit and atmospheric trajectory of the Peekskill meteorite from video records. *Nature* 367:624–626.
- Brown P., Hildebrand A. R., Zolensky M. E., Grady M., Clayton R. N., Mayeda T. K., Tagliaferri E., Spalding R., MacRae N. D., Hoffman E. L., Mittlefehldt D. W., Wacker J. F., Bird J. A., Campbell M. D., Carpenter R., Gingerich H., Glatiotis M., Greiner E., Mazur M. J., McCausland P. J. A., Plotkin H., and Mazur T. R. 2000. The fall, recovery orbit, and composition of the Tagish Lake meteorite: A new type of carbonaceous chondrite. *Science* 290:320–325.
- Ceplecha Z. 1961. Multiple fall of Příbram meteorites photographed. 1. Double-station photographs of the fireball and their relations to the found meteorites. *Bulletin of the Astronomical Institute of Czechoslovakia* 12:21–47.
- Ceplecha Z., Borovička J., Elford W. G., Revelle D. O., Hawkes R. L., Porubcan V., and Simek M. 1998. Meteor phenomena and bodies. *Space Science Reviews* 84:327–471.
- Fomenkova M. N., Kerridge J. F., Marti K., and McFadden L. A. 1992. Compositional trends in rock-forming elements of Comet Halley dust. *Science* 258:266–269.
- Greenberg J. M. 1998. From comets to meteors. *Earth, Moon, and Planets* 82–83:313–324.
- Halliday I. 1961. A study of spectral line identifications in Perseid meteor spectra. *Publications of the Dominion Observatory* 25:3–16.
- Halliday I., Griffin A. A., and Blackwell A. T. 1996. Detailed data for 259 fireballs from the Canadian camera network and inferences concerning the influx of large meteoroids. *Meteoritics & Planetary Science* 31:185–217.
- Hawkes R. L. and Jones J. 1975. A quantitative model for the ablation of dustball meteors. *Monthly Notices of the Royal Astronomical Society of London* 173:339–356.
- Howat I. D., Murray J., Mills D., and Berry D. S. 1996. Starlink User Note 50.19. Rutherford Appleton Laboratory.
- Hughes D. 1993. Meteoroids: An overview. In *Meteoroids and their parent bodies, Proceedings of the International Astronomical Symposium*, edited by Stollh J. and Williams I. P. Bratislava: Astronomical Institute, Slovak Academy of Sciences.
- Jessberger E. K., Christoforidis A., and Kissel A. 1988. Aspects of the major element composition of Halley's dust. *Nature* 322:691–695.
- Jessberger E. K., Kissel J., and Rahe J. 1988b. The composition of comets. In *Origin and evolution of planetary and satellite atmospheres*. Tucson: University of Arizona Press. pp. 167–191.
- Kurucz R. L. 1991. *Precision photometry: Astrophysics of the galaxy*, edited by David Philip A. G., Upgren A. R., and Janes K. A. Schenectady: L. Davis Press. 386 p.
- McCrosky R. E., A. Posen, Schwartz G., and Shao C. Y. 1971. Lost City meteorite: Its recovery and a comparison with other fireballs. *Journal of Geophysical Research* 76:4090–4108.
- Ozawa K. and Nagahara H. 2000. Kinetics of diffusion-controlled evaporation of Fe-Mg olivine: Experimental study and implication for stability of Fe-rich olivine in the solar nebula. *Geochimica et Cosmochimica Acta* 64:939–955.
- Rendtel J. 1993. Handbook for photographic meteor observations. International Meteor Organization Monograph No. 3. Potsdam, Germany.
- Rietmeijer F. J. M. 1998. Interplanetary dust particles. In *Planetary materials*, edited by Papike J. J. Washington D.C.: Mineralogical Society of America. pp. 1–95.
- Rietmeijer F. J. M. 2000. Shower meteoroids: Constraints from interplanetary dust particles and Leonid meteors. *Earth, Moon, and Planets* 88:35–58.
- Rietmeijer F. J. M. and Jenniskens P. 1998. Recognizing Leonid meteoroids among the collected stratospheric dust. *Earth, Moon, and Planets* 82–83:505–524.
- Rietmeijer F. J. M. and Nuth J. A., III. 1998. Collected extraterrestrial materials: Constraints on meteor and fireball compositions. *Earth, Moon, and Planets* 82–83:325–350.
- Rietmeijer F. J. M. 2001. Identification of Fe-rich meteoric dust. *Planetary and Space Science* 49:71–77.
- Rietmeijer F. J. M. 2002. The earliest chemical dust evolution in the solar nebula. *Chemie der Erde* 62:1–45.
- Spurny P., Heinlein D., and Oberst J. 2002. The atmospheric trajectory and heliocentric orbit of the Neuschwanstein meteorite fall on April 6, 2002. Proceedings, Asteroids, Comets, Meteors 2002.
- Trigo-Rodríguez J. M. 2002. Spectroscopic analysis of cometary and asteroidal fragments during their entry into the terrestrial atmosphere. PhD thesis, University of Valencia, Spain. In Spanish.
- Verniani F. 1973. An analysis of the physical parameters of 5759 faint radio meteors. *Journal of Geophysical Research* 78:8429–8462.